Axion Dark Matter : Motivation and Search Techniques

Pierre Sikivie

UCLA DM Conference
February 17, 2016

- Motivation

Axions solve the strong CP problem

Axions are present in many models of beyond-the-Standard Model physics

Axions are a form of cold dark matter

Axion BEC explains the existence and properties of caustic rings in galactic halos

- Axion Search Techniques

  the cavity haloscope

  the axion helioscope

  shining light through walls

  NMR methods

  axion mediated long-range forces

  LC circuit

  atomic transitions

The Strong CP Problem

$$L_{\mathrm{QCD}} = \ \ldots + \bar{\theta}\,\frac{g^2}{32\,\pi^2}\,G^a{}_{\mu\nu}\,\tilde{G}^{a\mu\nu}$$

where

$$\bar{\theta} = \theta - \arg\left(m_u\, m_d \ \ldots \ m_t\right)$$
$$= \theta - \arg\det\left(Y^u\, Y^d\right)$$

The absence of P and CP violation in the strong interactions requires

$$\bar{\theta} \leq 10^{-10}$$

from upper limit
on the neutron electric
dipole moment

If a $U_{PQ}(1)$ symmetry is assumed,

$$L = \ldots + \frac{a}{f_a}\frac{g^2}{32\pi^2} G^a{}_{\mu\nu} \tilde{G}^{a\mu\nu} + \frac{1}{2}\partial_\mu a\, \partial^\mu a + \ldots$$

$\bar{\theta} = \dfrac{a}{f_a}$ relaxes to zero,

and a light neutral pseudoscalar particle is predicted: the axion.

Weinberg, Wilczek 1978

$$m_a \; ; \quad 6 \text{ eV } \frac{10^6 \text{ GeV}}{f_a}$$

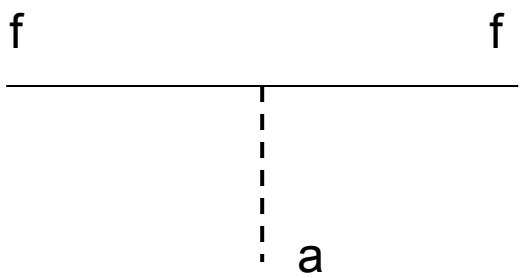

$$\mathcal{L}_{a\bar{f}f} = i g_f \frac{a}{f_a} \bar{f} \gamma_5 f$$

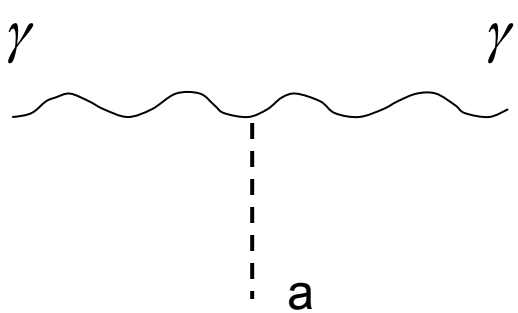

$$\mathcal{L}_{a\gamma\gamma} = g_\gamma \frac{a}{f_a} \vec{E} \cdot \vec{B}$$

g_γ = 0.97 in KSVZ model
0.36 in DFSZ model

The remaining axion window

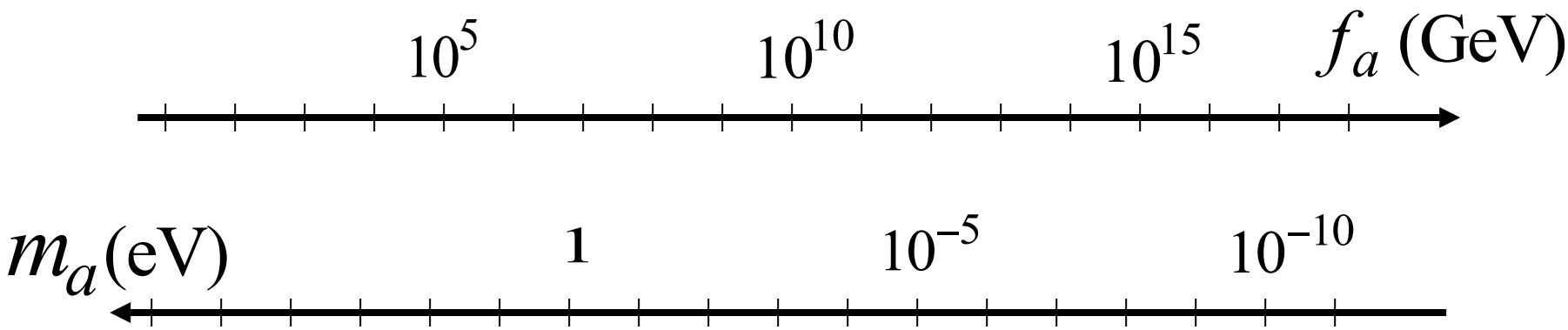

laboratory searches

cosmology

stellar evolution

Axion production by vacuum realignment

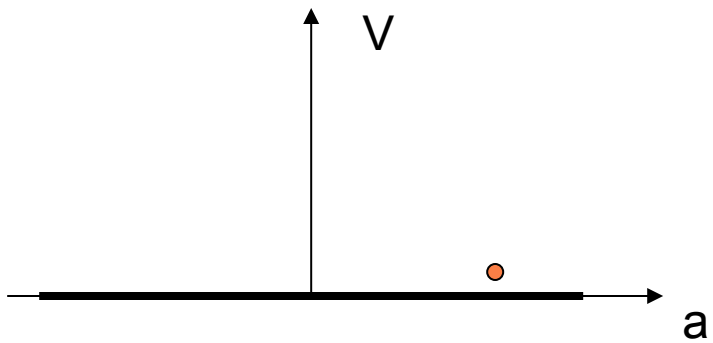

$T \geq 1\,\mathrm{GeV}$

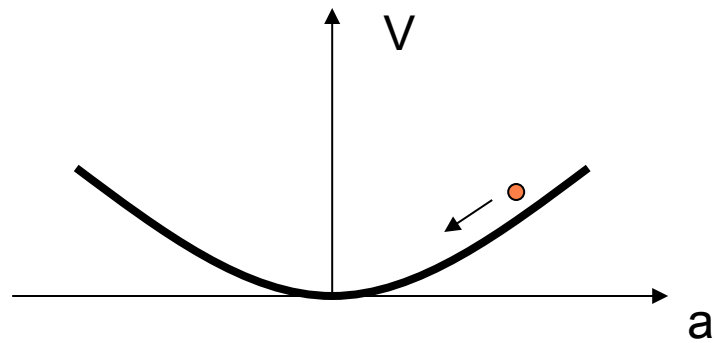

$T \leq 1\,\mathrm{GeV}$

$$n_a(t_1) \;;\; \frac{1}{2} m_a(t_1)\, a(t_1)^2 \;;\; \frac{1}{2t_1} f_a^{\,2}\, \alpha(t_1)^2$$

initial misalignment angle

$$\rho_a(t_0) \;;\; m_a\, n_a(t_1) \left(\frac{R_1}{R_0} \right)^3 \propto m_a^{\,-\frac{7}{6}}$$

J. Preskill, M. Wise & F. Wilczek, L. Abbott & PS, M. Dine & W. Fischler, 1983

Cold axion properties

- number density

$$n(t) \;:\; \frac{4\cdot 10^{47}}{\mathrm{cm}^3}\left(\frac{f_a}{10^{12}\,\mathrm{GeV}}\right)^{\frac{5}{3}}\left(\frac{a(t_1)}{a(t)}\right)^3$$

- velocity dispersion

$$\delta \mathrm{v}(t) \;:\; \frac{1}{m_a\, t_1}\,\frac{a(t_1)}{a(t)}$$

if decoupled

- phase space density

$$\mathcal{n} \;:\; n(t)\,\frac{(2\pi)^3}{\frac{4\pi}{3}(m_a\,\delta \mathrm{v})^3} \;:\; 10^{61}\left(\frac{f_a}{10^{12}\,\mathrm{GeV}}\right)^{\frac{8}{3}}$$

Bose-Einstein Condensation

if identical bosonic particles
are highly condensed in phase space
and their total number is conserved
and they thermalize

then most of them go to the lowest energy
available state

why do they do that?

by yielding their energy to the non-condensed particles, the total entropy is increased.

the axions thermalize and form a BEC after a time τ

$t < \tau$

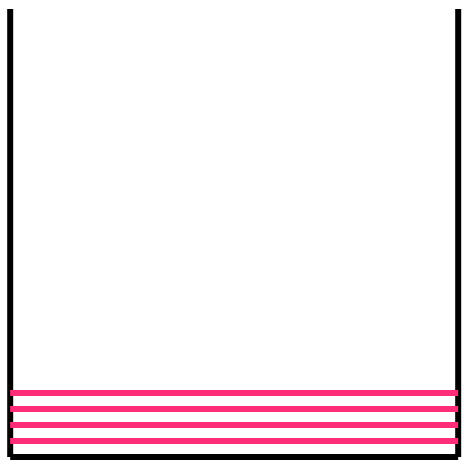

the axion fluid obeys classical field equations, behaves like CDM

$t > \tau$

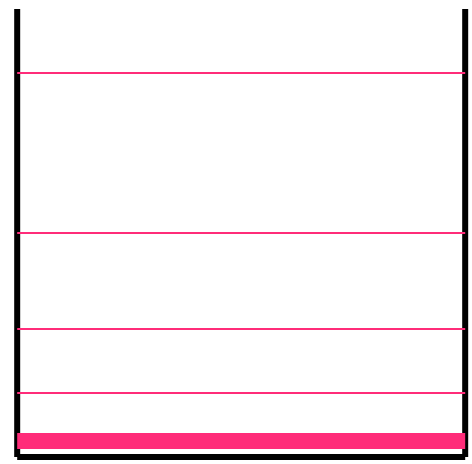

the axion fluid does not obey classical field equations, does not behave like CDM

Quantum axion field dynamics

$$H = \sum_j \omega_j a_j^\dagger a_j \quad + \quad \sum_{ijkl} \frac{1}{4} \Lambda_{kl}^{ij} a_k^\dagger a_l^\dagger a_i a_j$$

O. Erken et al., PRD 85 (2012) 063520

From $\frac{1}{4!}\lambda\phi^4$ self-interactions

$$\Lambda_\lambda{}^{\vec{p}_3,\vec{p}_4}_{\vec{p}_1,\vec{p}_2} = -\frac{\lambda}{4m^2V}\,\delta_{\vec{p}_1+\vec{p}_2,\vec{p}_3+\vec{p}_4}$$

From gravitational self-interactions

$$\Lambda_g{}^{\vec{p}_3,\vec{p}_4}_{\vec{p}_1,\vec{p}_2} = -\frac{4\pi G m^2}{V}\,\delta_{\vec{p}_1+\vec{p}_2,\vec{p}_3+\vec{p}_4}\left(\frac{1}{|\vec{p}_1-\vec{p}_3|^2}+\frac{1}{|\vec{p}_1-\vec{p}_4|^2}\right)$$

After t_1 , axions thermalize in the "condensed" regime

$$\Gamma \; >> \; \delta E$$

$$\frac{d}{dt}\mathcal{N}_l = i \sum_{ijk} \frac{1}{2}(\Lambda^{kl}_{ij} a^\dagger_i a^\dagger_j a_k a_l - h.c.)$$

implies $\Gamma \sim \frac{1}{4} n \lambda m^{-2}$ for $\lambda \phi^4$

and $\Gamma \sim 4\pi G n m^2 \ell^2$ for self-gravity

$(\ell \equiv 1/\delta p)$

Thermalization occurs due to gravitational interactions

PS + Q. Yang, PRL 103 (2009) 111301

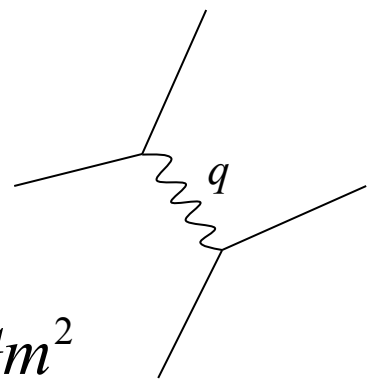

$$\frac{Gm^2}{q^2}$$

$$\Gamma_g \sim 4\pi G n m^2 l^2 \qquad \text{with } l = (m\,\delta \mathrm{v})^{-1}$$

$$\sim 5 \cdot 10^{-7} H(t_1) \left(\frac{f}{10^{12}\ \mathrm{GeV}} \right)^{\frac{2}{3}}$$

at time t_1

$$\Gamma_g(t)/H(t) \propto t\, a(t)^{-1} \propto a(t)$$

Gravitational interactions thermalize the axions and cause them to form a BEC when the photon temperature

$$T_\gamma \sim 500 \text{ eV} \left(\frac{f}{10^{12} \text{ GeV}} \right)^{\frac{1}{2}}$$

After that

$$\delta \mathrm{v} : \frac{1}{m\,t}$$

$$\Gamma_g(t) / H(t) \propto t^3 \, a(t)^{-3}$$

Axion BEC thermalization has also been discussed by

- Saikawa and Yamaguchi, Phys. Rev. D87 (2015) 085010
- S. Davidson and Elmer, JCAP 1312 (2013) 034
- J. Berges and J. Jaeckel, Phys. Rev. D91 (2015) 025020
- A. Guth, M.P. Hertzberg and C. Prescod-Weinstein, Phys. Rev. D92 (2015) 103513

Guth et al. write: " ... we conclude that while a Bose-Einstein condensate is formed, the claim of long-range correlation is unjustified."

the axion BEC is inhomogeneous because it is gravitationally unstable. However it does have the long range correlations that are characteristic of BEC. The BEC correlation length is not to be identified with the scale of homogeneity.

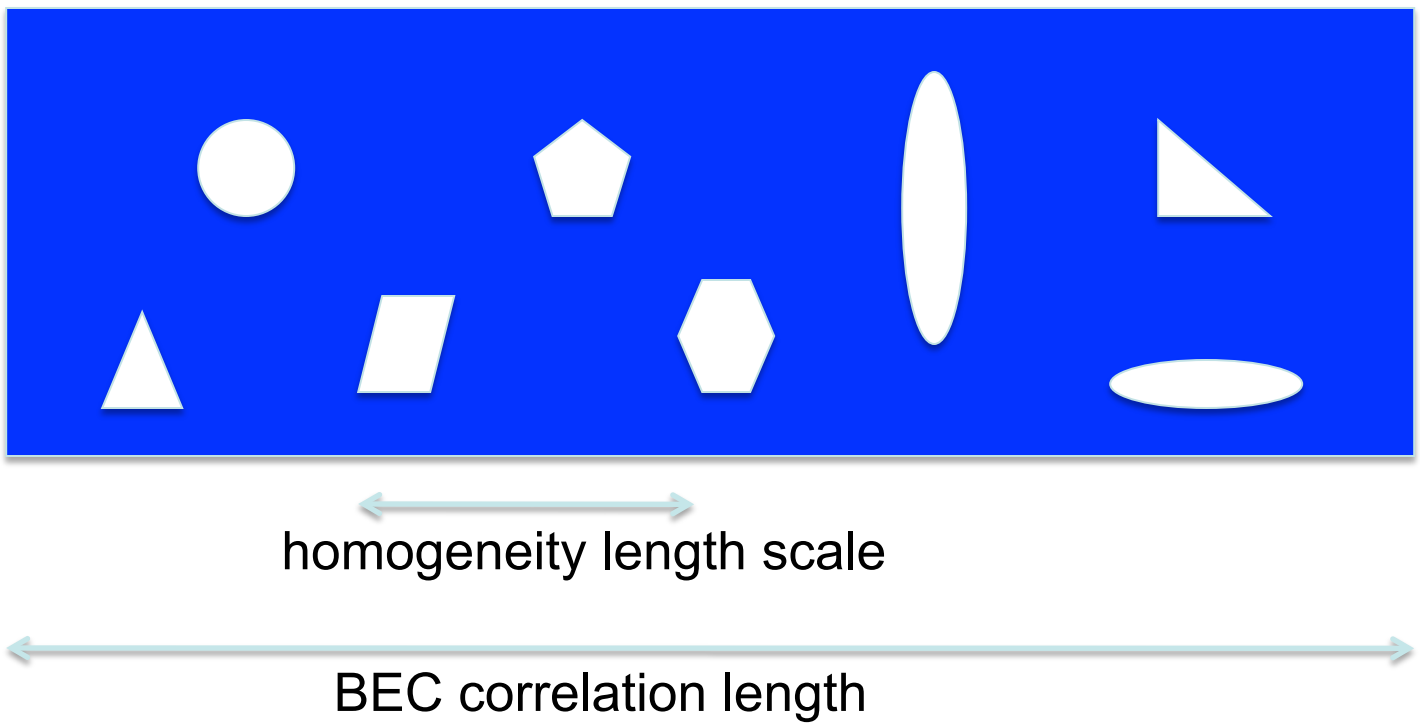

Tidal torque theory

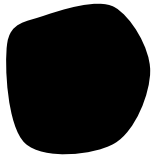

neighboring
protogalaxy

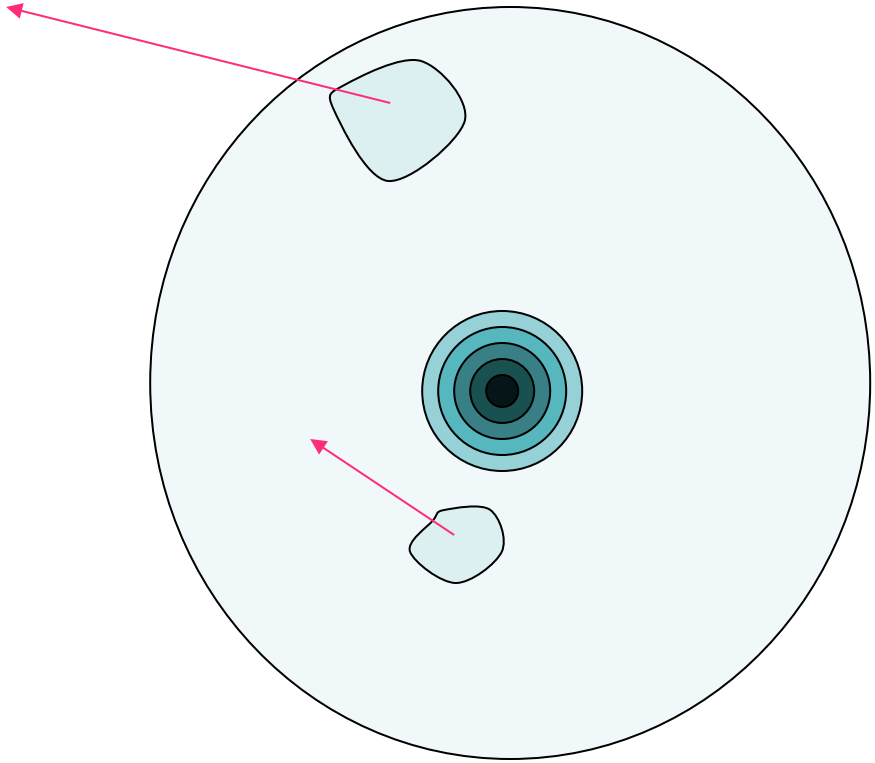

Stromberg 1934; Hoyle 1947; Peebles 1969, 1971

Tidal torque theory with ordinary CDM

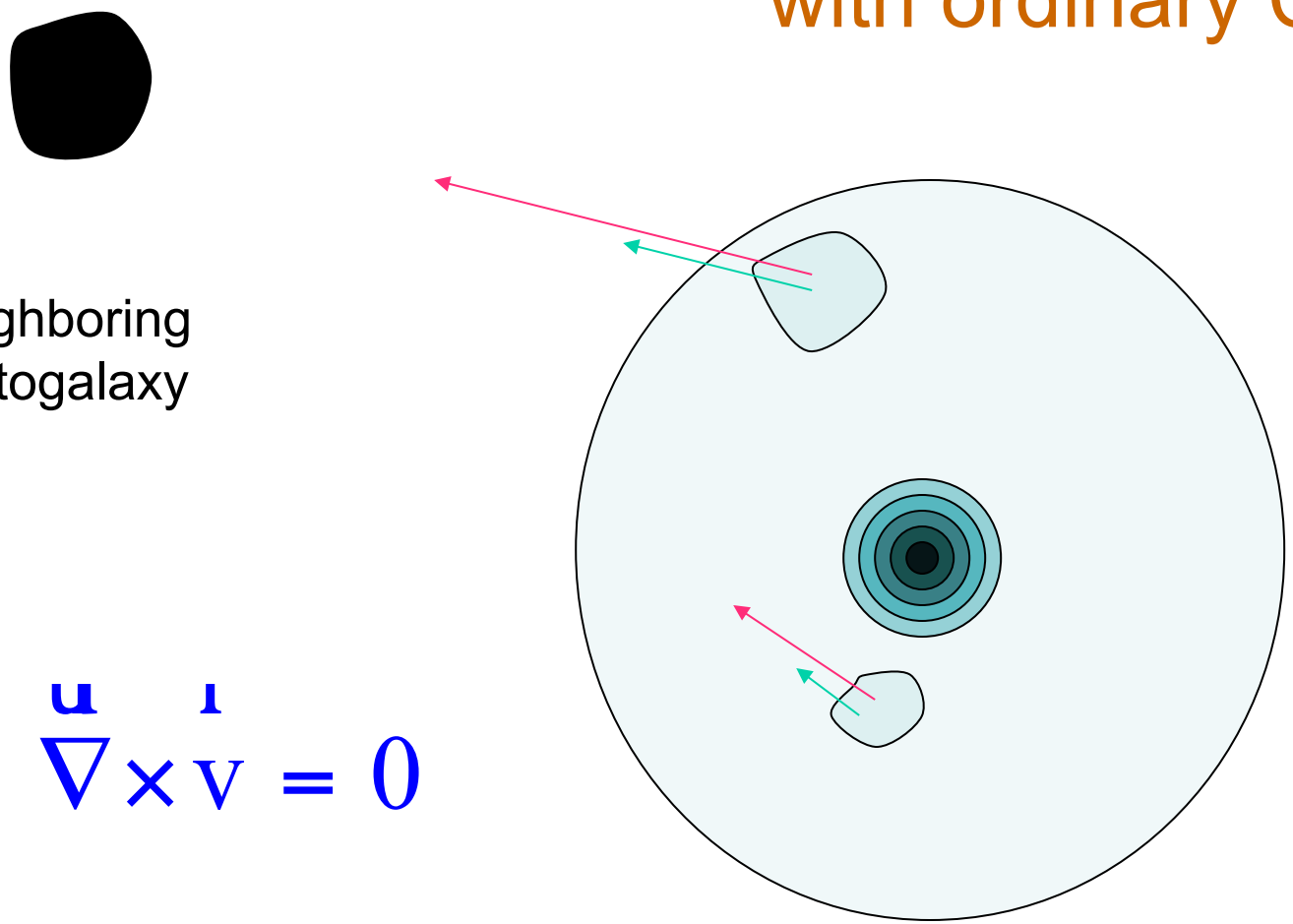

$$\vec{\nabla} \times \vec{v} = 0$$

the velocity field remains irrotational

Tidal torque theory with axion BEC

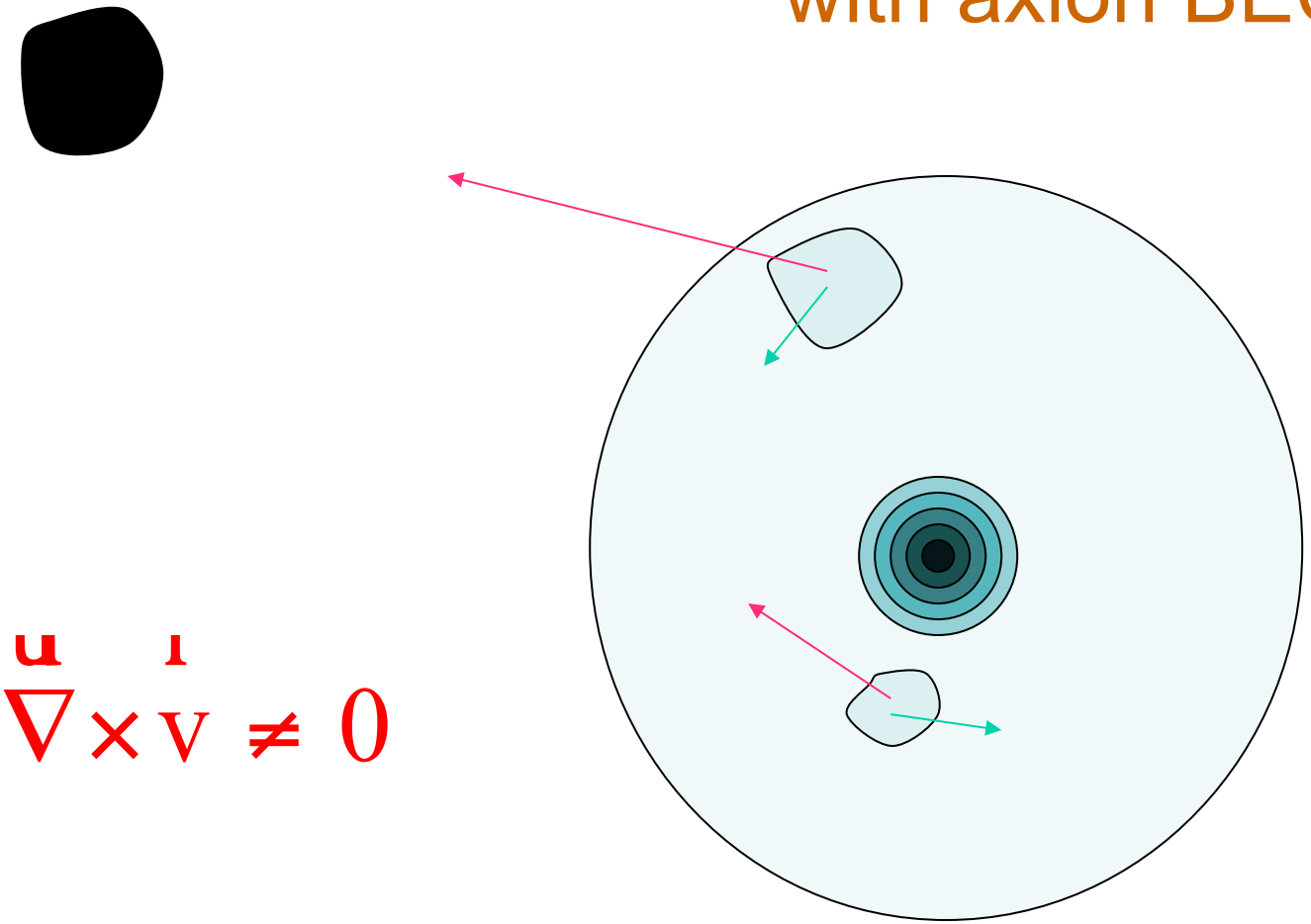

$$\vec{\nabla} \times \vec{v} \neq 0$$

in their lowest energy available state, the axions fall in with net overall rotation

simulation by Arvind Natarajan

in case of net overall rotation

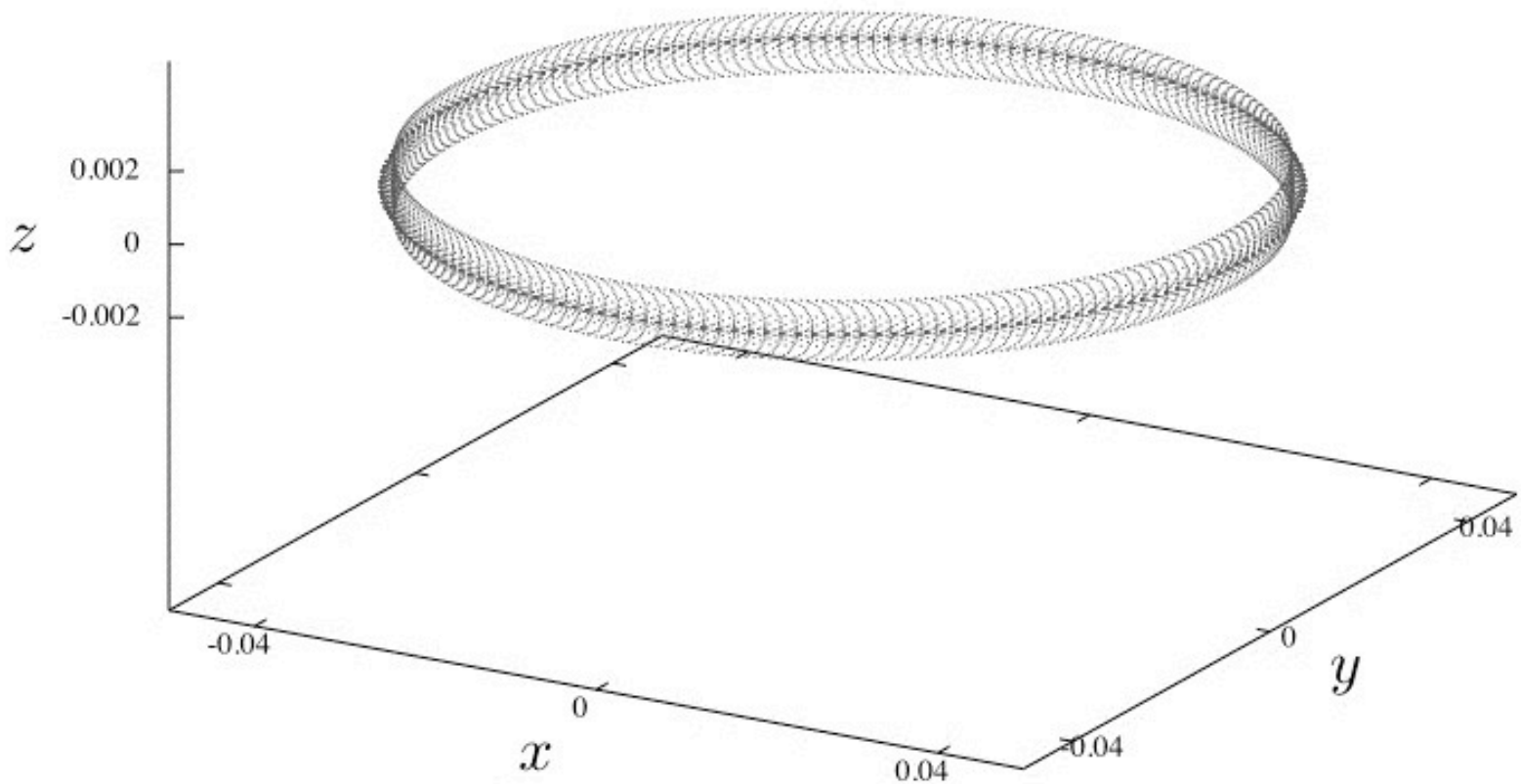

The caustic ring cross-section

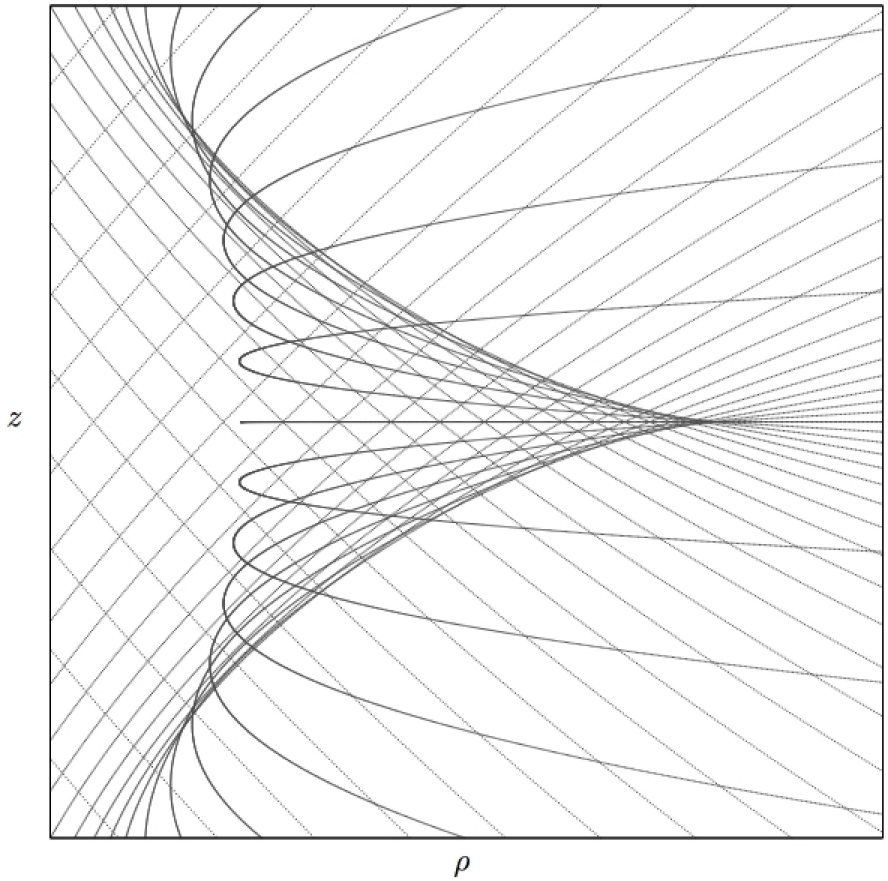

D_{-4}

an elliptic umbilic catastrophe

On the basis of the self-similar infall model (Filmore and Goldreich, Bertschinger) with angular momentum (Tkachev, Wang + PS), the caustic rings were predicted to be

in the galactic plane

with radii $(n = 1, 2, 3 \ldots)$

$$a_n = \frac{40\text{kpc}}{n}\left(\frac{v_{rot}}{220\text{km/s}}\right)\left(\frac{j_{max}}{0.18}\right)$$

$j_{max} \cong 0.18$ was expected for the Milky Way halo from the effect of angular momentum on the inner rotation curve.

- Axion Search Techniques

  the cavity haloscope

  the axion helioscope

  shining light through walls

  NMR methods

  axion mediated long-range forces

  LC circuit

  atomic transitions

Axion dark matter is detectable

PS '83

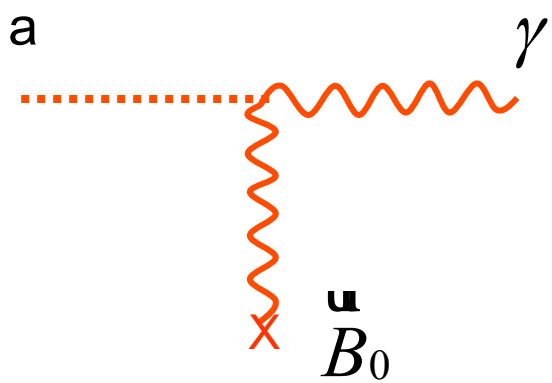

$$\mathcal{L}_{a\gamma\gamma} = g_\gamma \frac{a}{f_a} \vec{E} \cdot \vec{B}$$

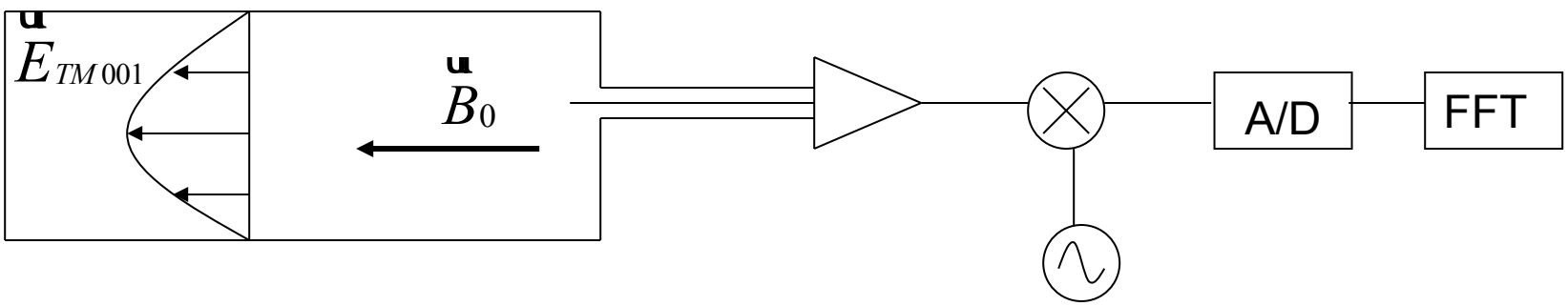

$$h\nu = m_a c^2 \left(1 + \frac{1}{2}\beta^2\right)$$

$$\beta = \frac{v}{c} : 10^{-3}$$

$$Q_a : 10^6$$

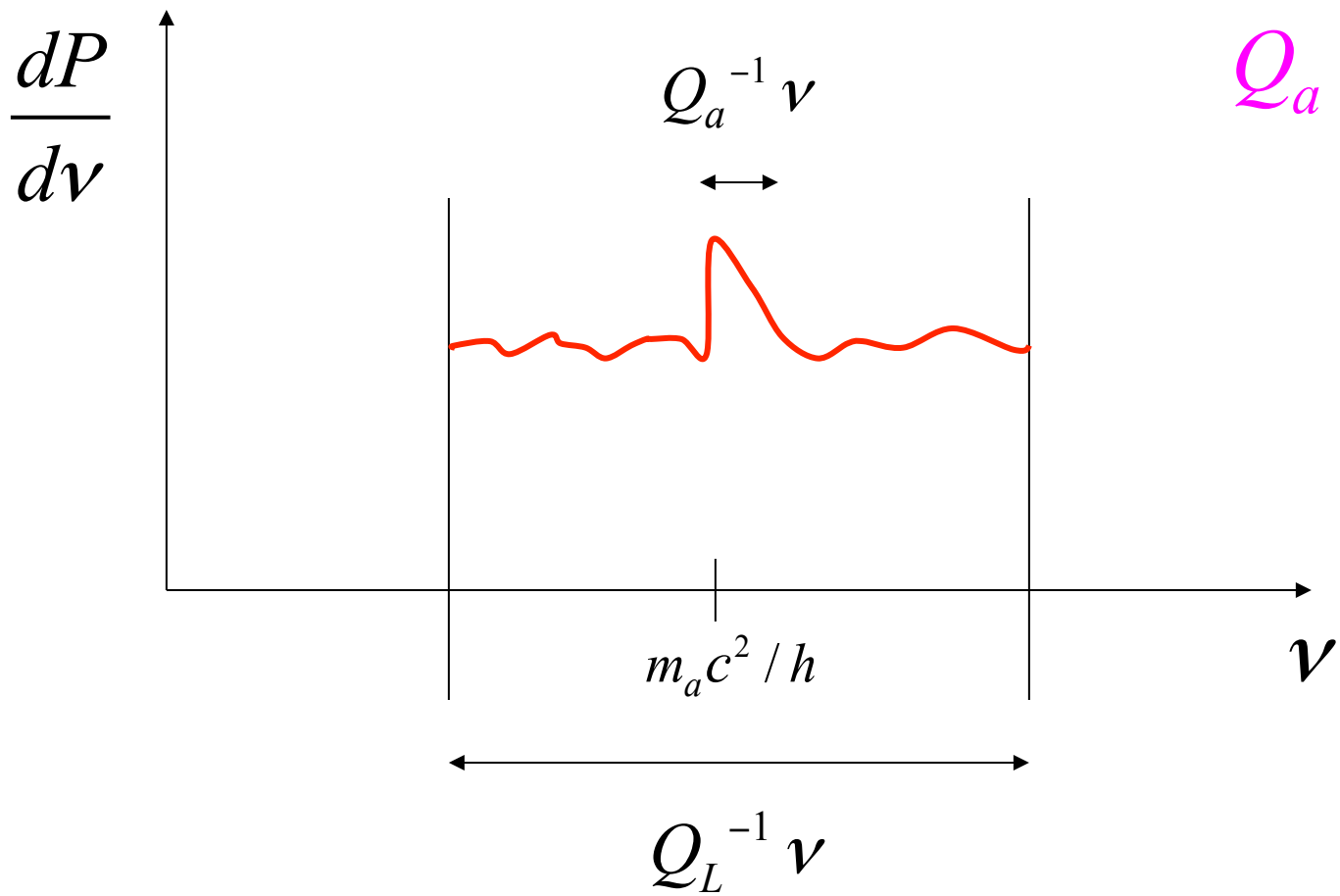

Axion Dark Matter eXperiment

see talks here by G. Carosi and B. Brubaker

Magnet with Insert (side view)

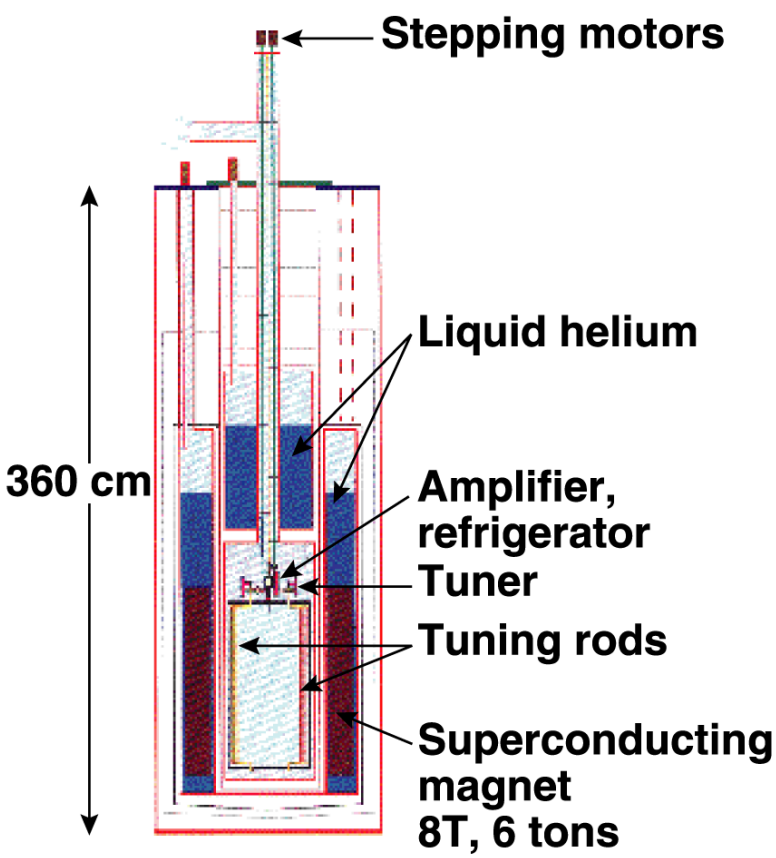

Pumped LHe → T ~ 1.5 k

Magnet

8 T, 1 m × 60 cm ∅

Gen 2 ADMX sensitivity

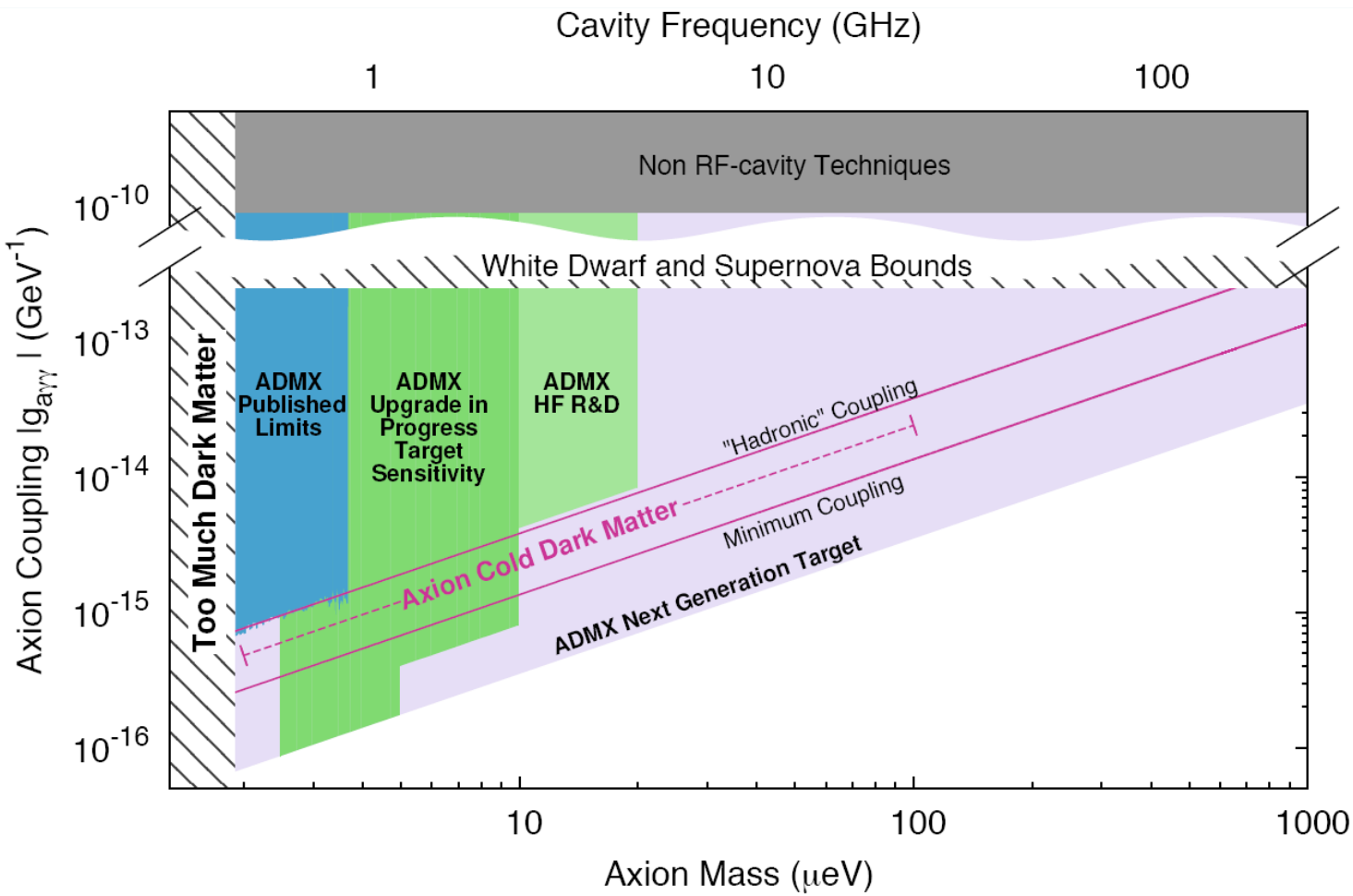

Will scan the lower-mass decade at or below DFSZ sensitivity

Axion to photon conversion in a magnetic field

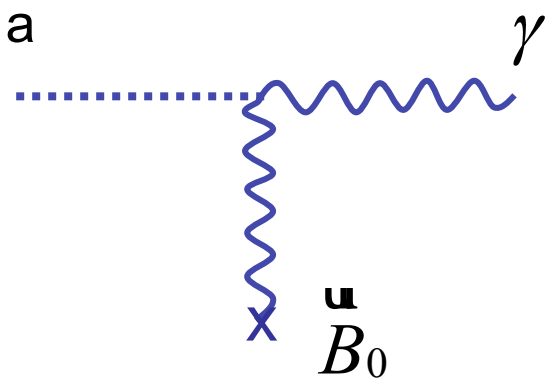

conversion probability

$$p(a \longleftrightarrow \gamma) = \left(\frac{\alpha\, g_\gamma}{\pi\, f_a}\right)^2 \mathrm{B}_0{}^2 \left(\frac{\sin\frac{q_z L}{2}}{q_z}\right)^2$$

with $$q_z = \frac{m_a{}^2 - \omega_{\mathrm{pl}}{}^2}{2E_a}$$

Theory

- P. S. ’83
- L. Maiani, R. Petronzio and E. Zavattini ’86
- K. van Bibber et al. ’87
- G. Raffelt and L. Stodolsky, ‘88
- K. van Bibber et al. ’89

Experiment

- D. Lazarus et al. ’92
- R. Cameron et al. ‘93
- S. Moriyama et al. ’98, Y. Inoue et al. ’02
- K. Zioutas et al. 04
- E. Zavattini et al. 05

Tokyo Axion Helioscope

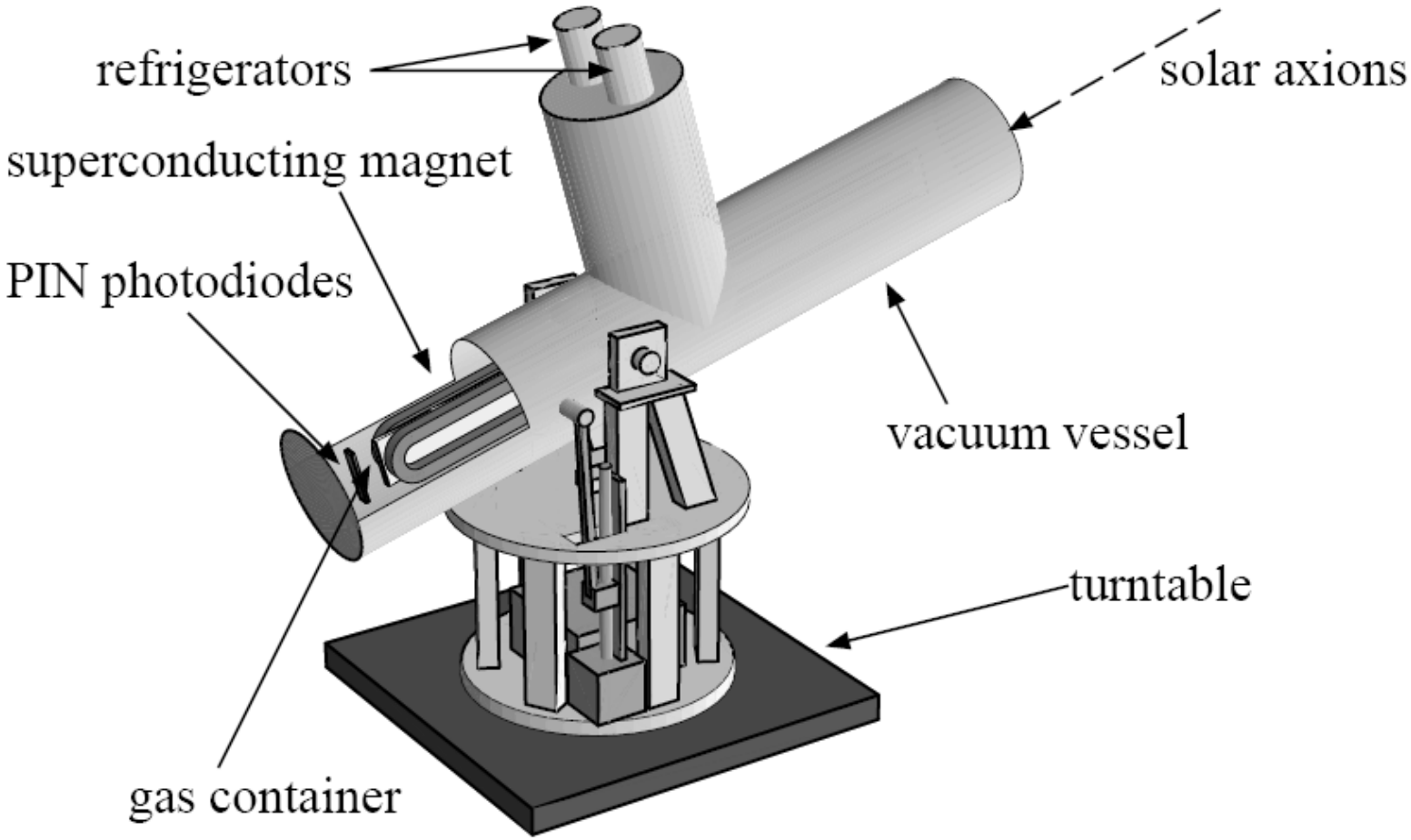


CAST
ANSALDO GIE
EUROPAMETALLI – LMI
E. ZANON

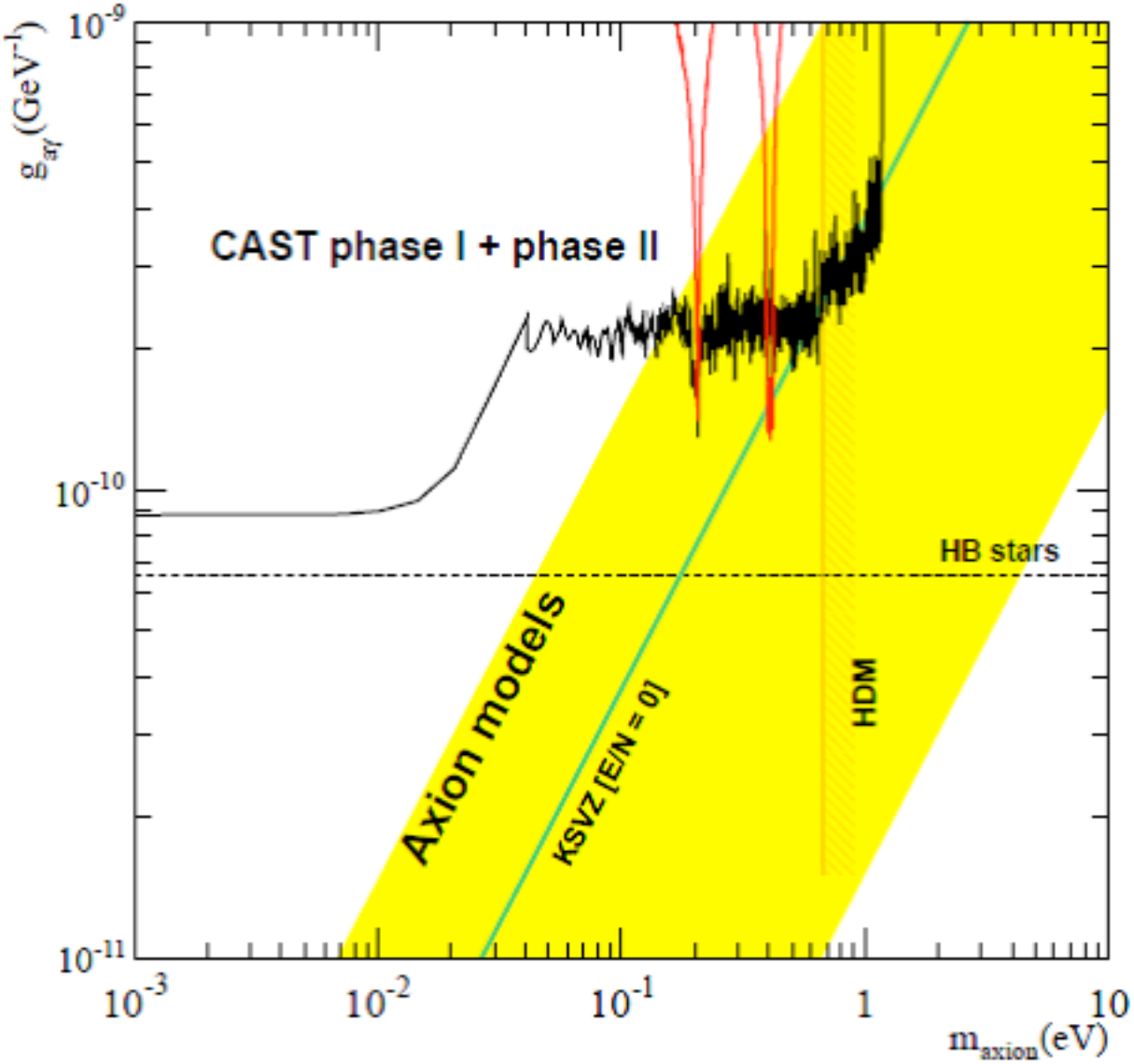

CAST Collaboration: Phys. Rev. Lett. 112 (2013) 091302

IAXO – Conceptual Design

- Large toroidal 8-coil magnet L = ~20 m
- 8 bores: 600 mm diameter each
- 8 x-ray optics + 8 detection systems
- Rotating platform with services

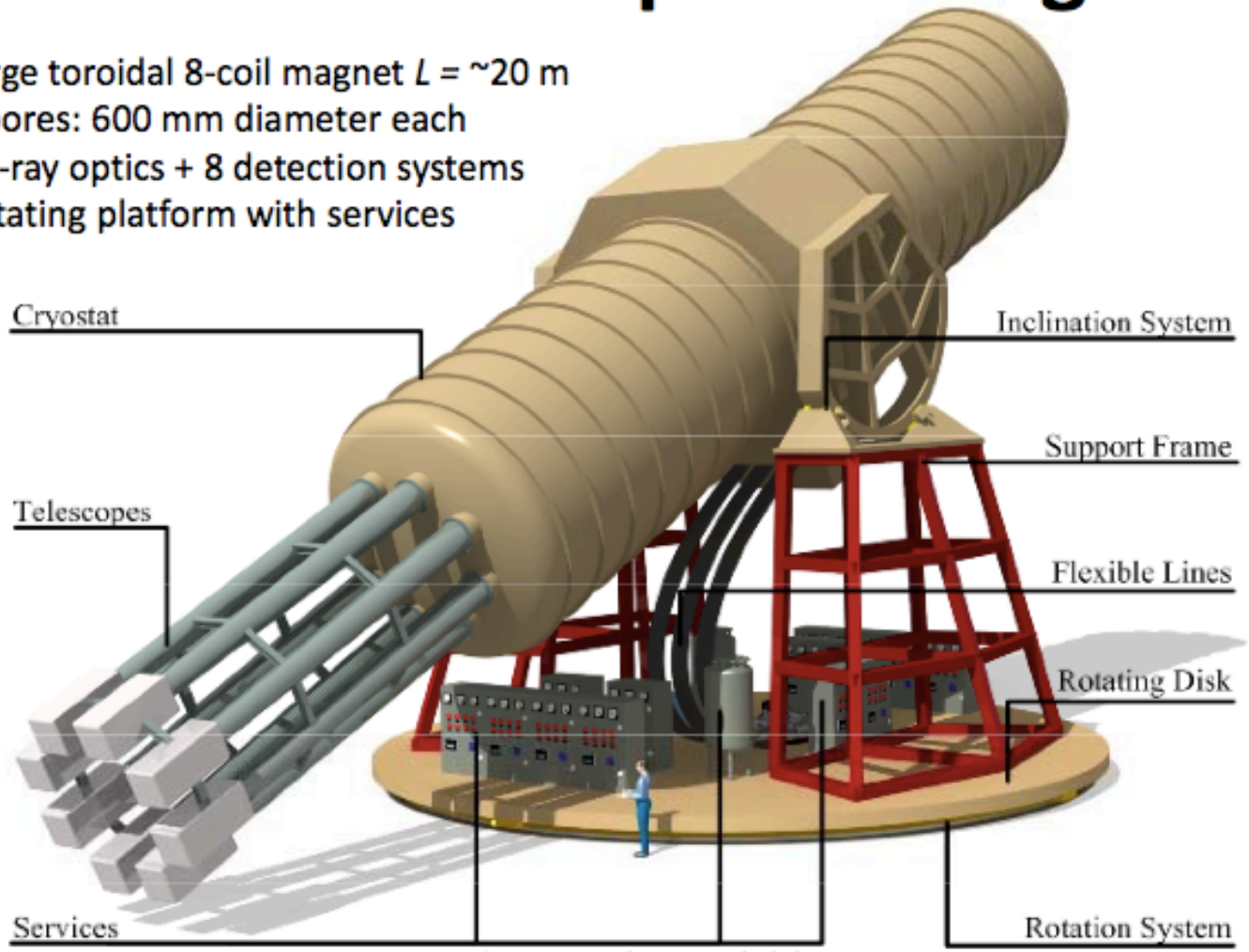

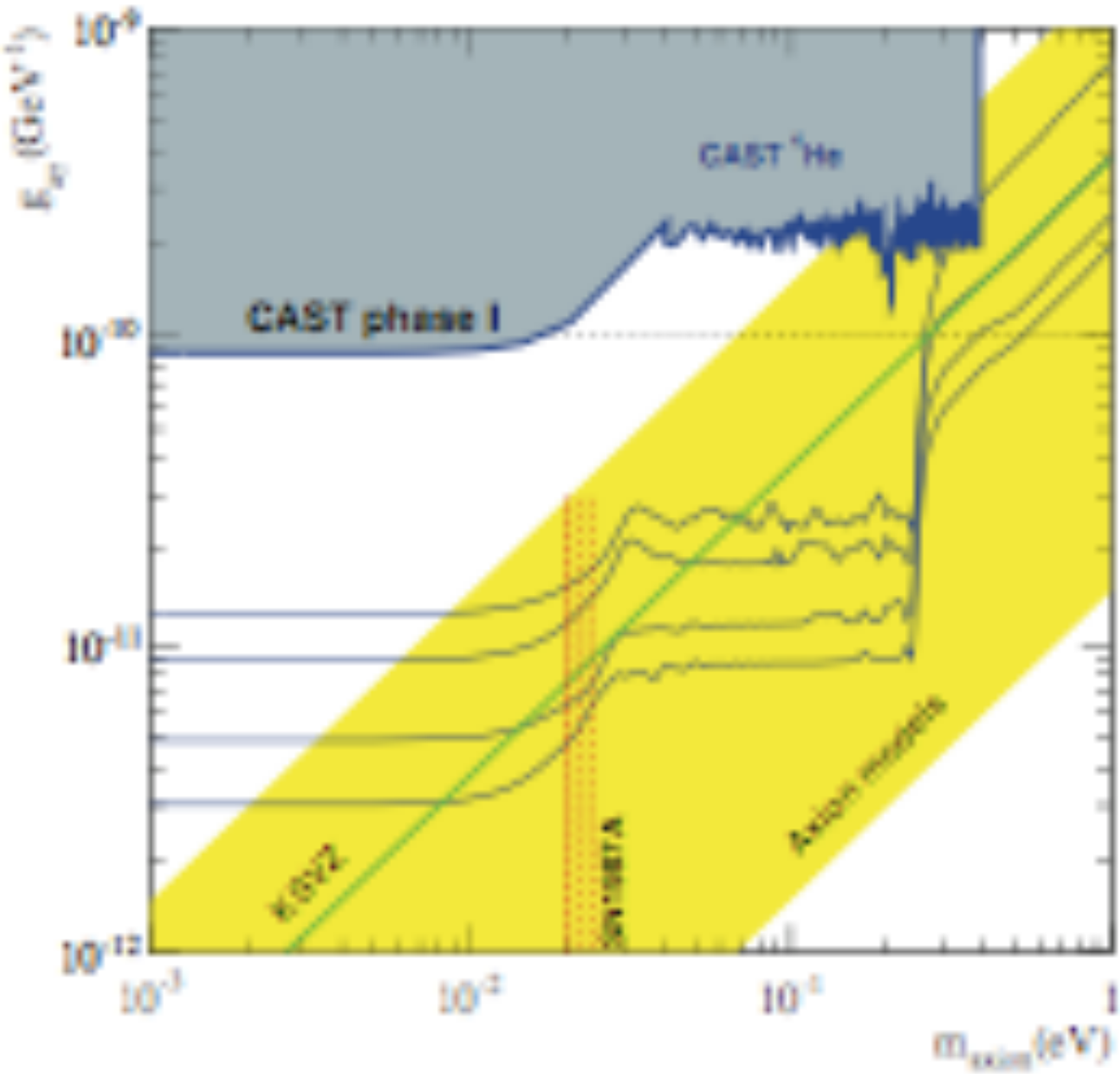
CAST phase I
CAST ^{3}He
KSVZ
DFSZ
Axion models
10^{-9}
10^{-10}
10^{-11}
10^{-12}
10^{-3}
10^{-2}
10^{-1}
1
m_{axion}(eV)

Shining light through walls

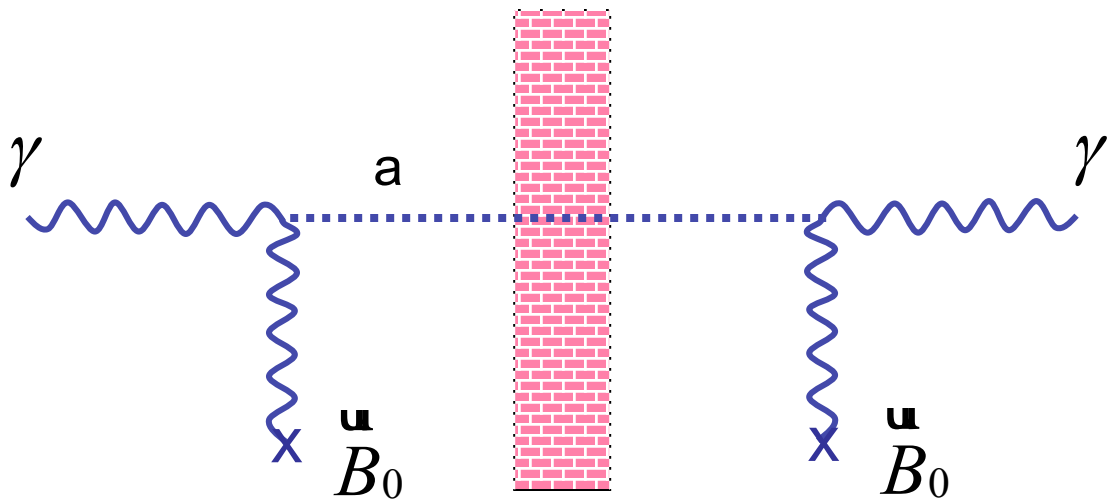

rate $\propto \dfrac{1}{f_a^{\,4}}$

K. van Bibber et al. ‘87

A. Ringwald ‘03

R. Rabadan,
A. Ringwald and
C. Sigurdson ‘05

P. Pugnat et al. '05

C. Robilliard et al. '07

A. Afanasev et al. '08

A. Chou et al. '08

K. Ehret et al. '10

Limits from "light through wall" axion searches

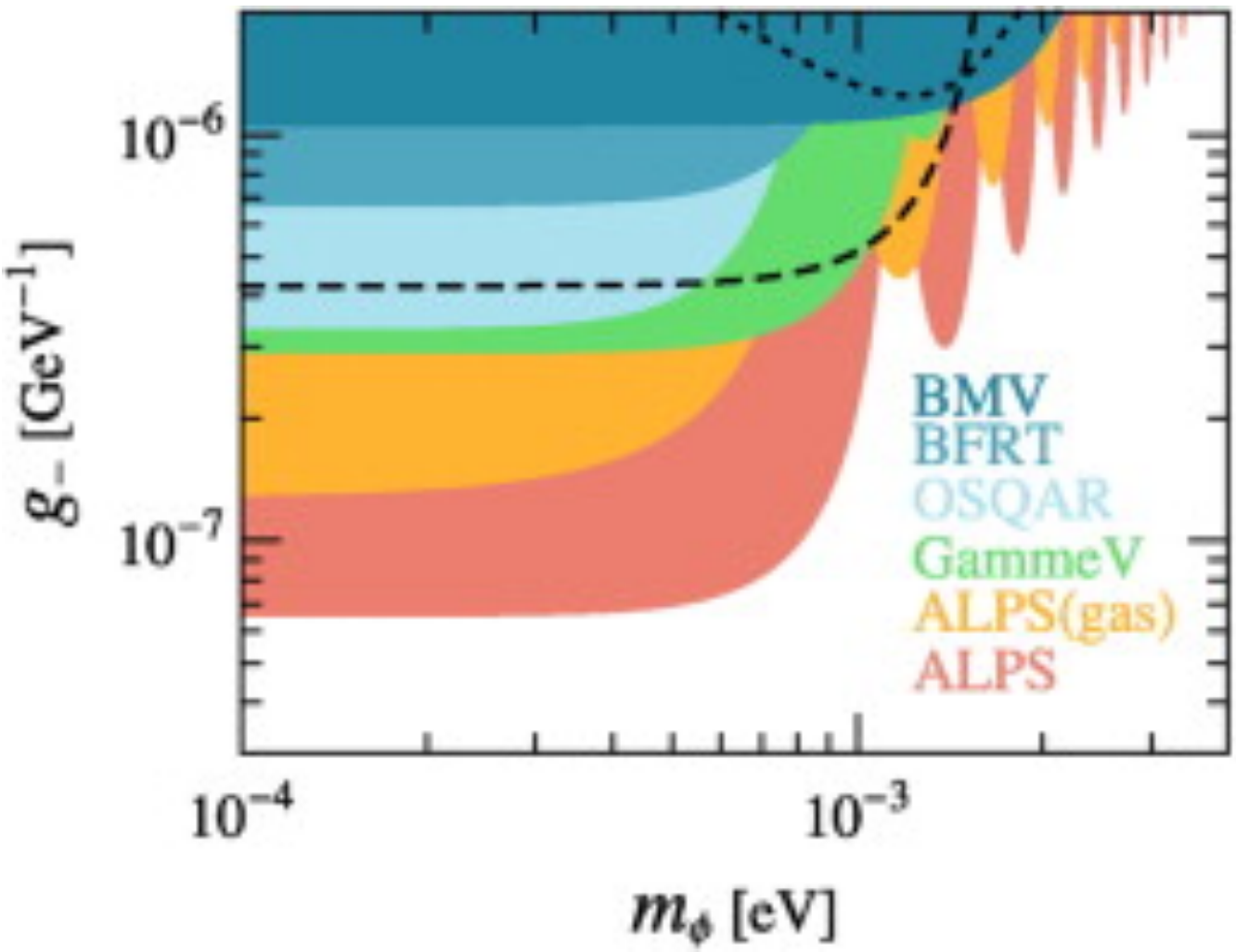

Resonantly Enhanced Axion-Photon Regeneration

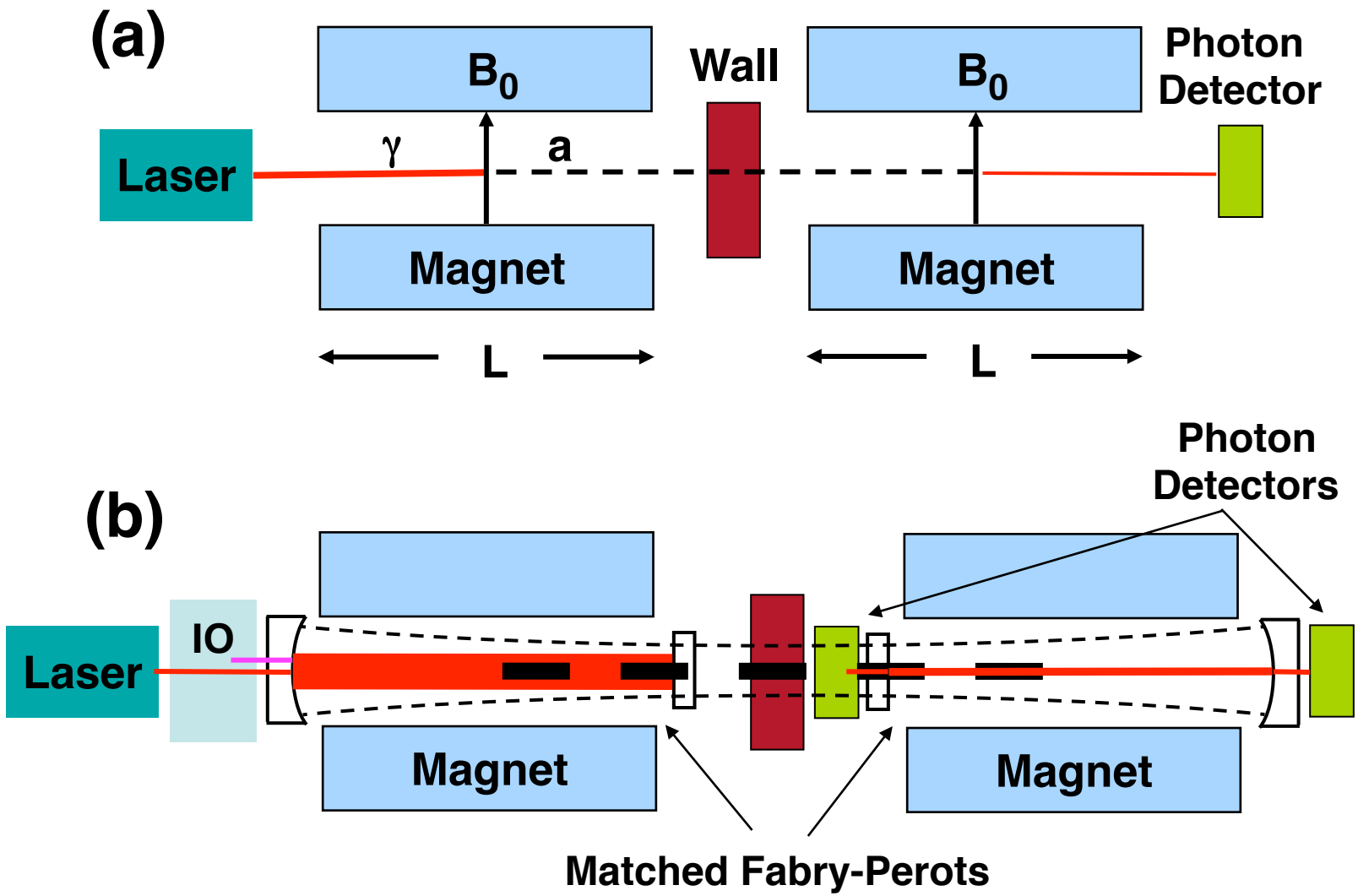

F. Hoogeveen (1996); P.S., D. Tanner and K. van Bibber (2007)

ALPS II at DESY

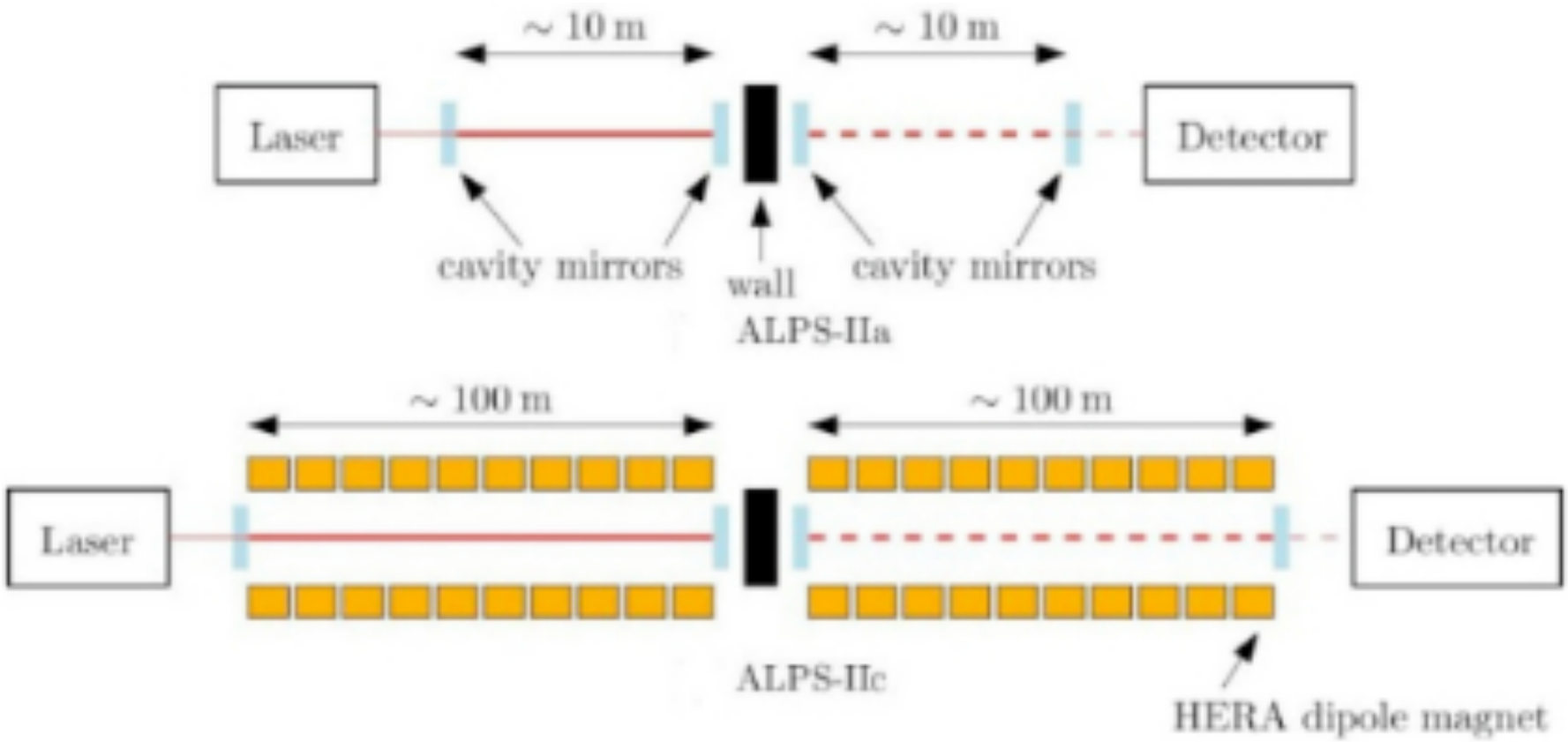

Expected sensitivity : $2 \cdot 10^{-11}\ \mathrm{GeV}^{-1}$

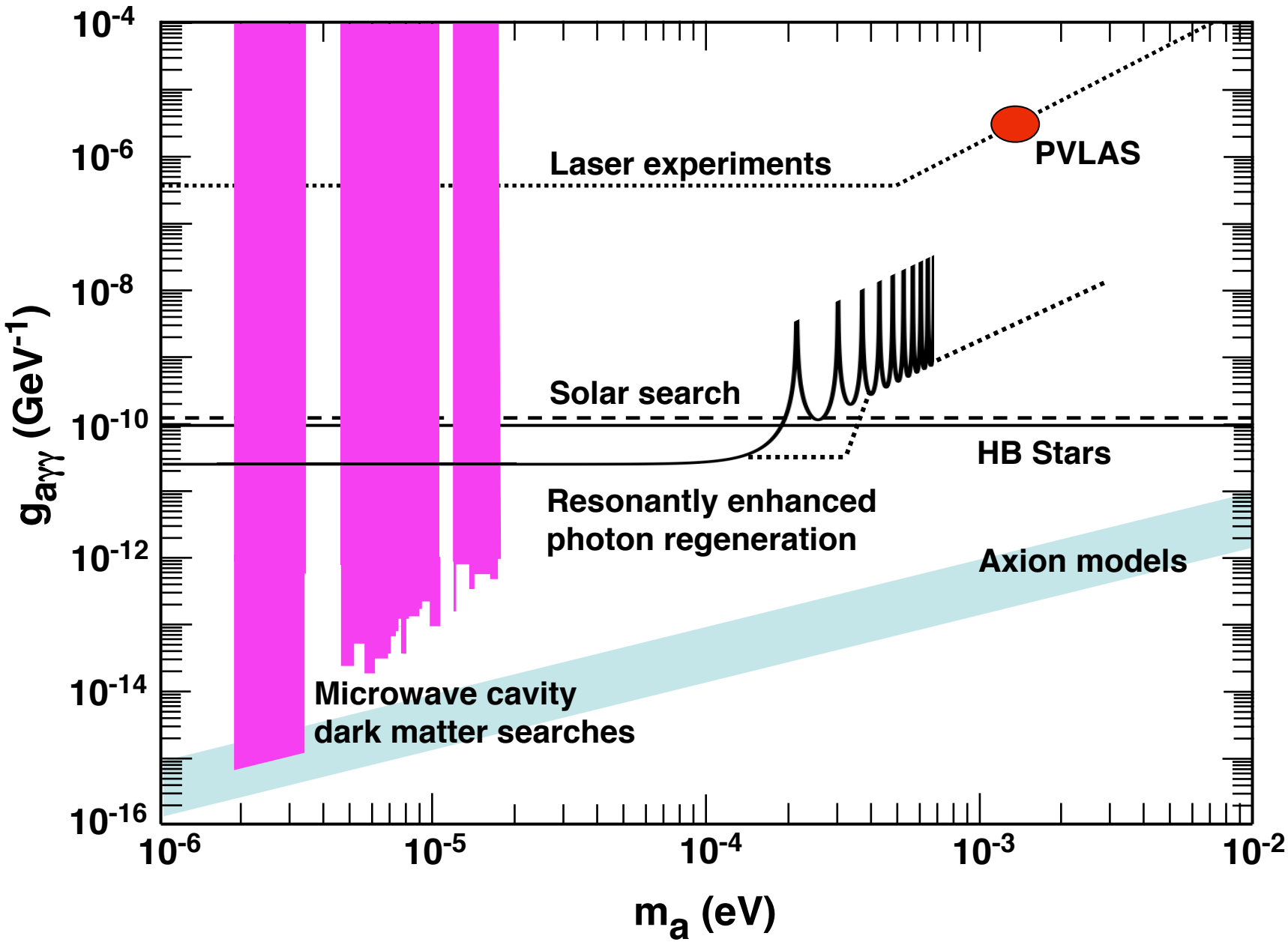
10^{-4}
10^{-6}
10^{-8}
10^{-10}
10^{-12}
10^{-14}
10^{-16}
$g_{a\gamma\gamma}$ (GeV^{-1})
Laser experiments
PVLAS
Solar search
HB Stars
Resonantly enhanced
photon regeneration
Axion models
Microwave cavity
dark matter searches
10^{-6}
10^{-5}
10^{-4}
10^{-3}
10^{-2}
m_a (eV)

Macroscopic forces mediated by axions

$$L_{a\bar{f}f} = g_f \frac{m_f}{f_a} a \bar{f} \left(i\gamma_5 + \theta_f \right) f$$

forces coupled to
the f spin density

forces coupled to
the f number density

background of
magnetic forces

$\vartheta_f : 10^{-17}$

Theory:

J. Moody and
F. Wilczek '84

Experiment:

A. Youdin et al. '96
W.-T. Ni et al. '96

NMR with long range axion field

A. Arvanitaki and A. Geraci, 2014

$$H_{\rm int} = \frac{g_f m_f \theta_f}{f_a} a(x)$$

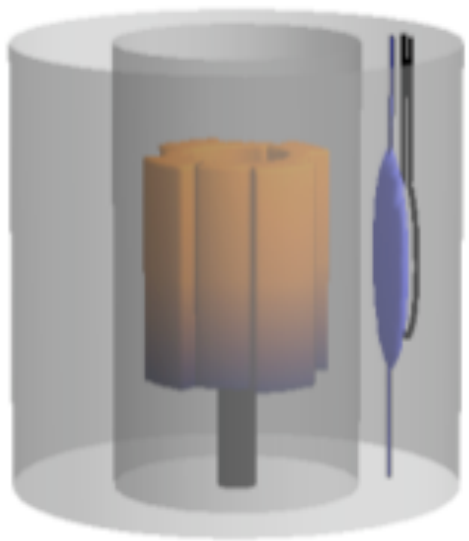

$$H_{\rm int} = \frac{g_f m_f}{f_a} \vec{\nabla} a(x) \cdot \vec{\sigma}$$

the rotating mass on the left produces an oscillating axion field

the oscillating axion field is an effective magnetic field in an NMR experiment

$$\omega = \gamma_N B_0$$

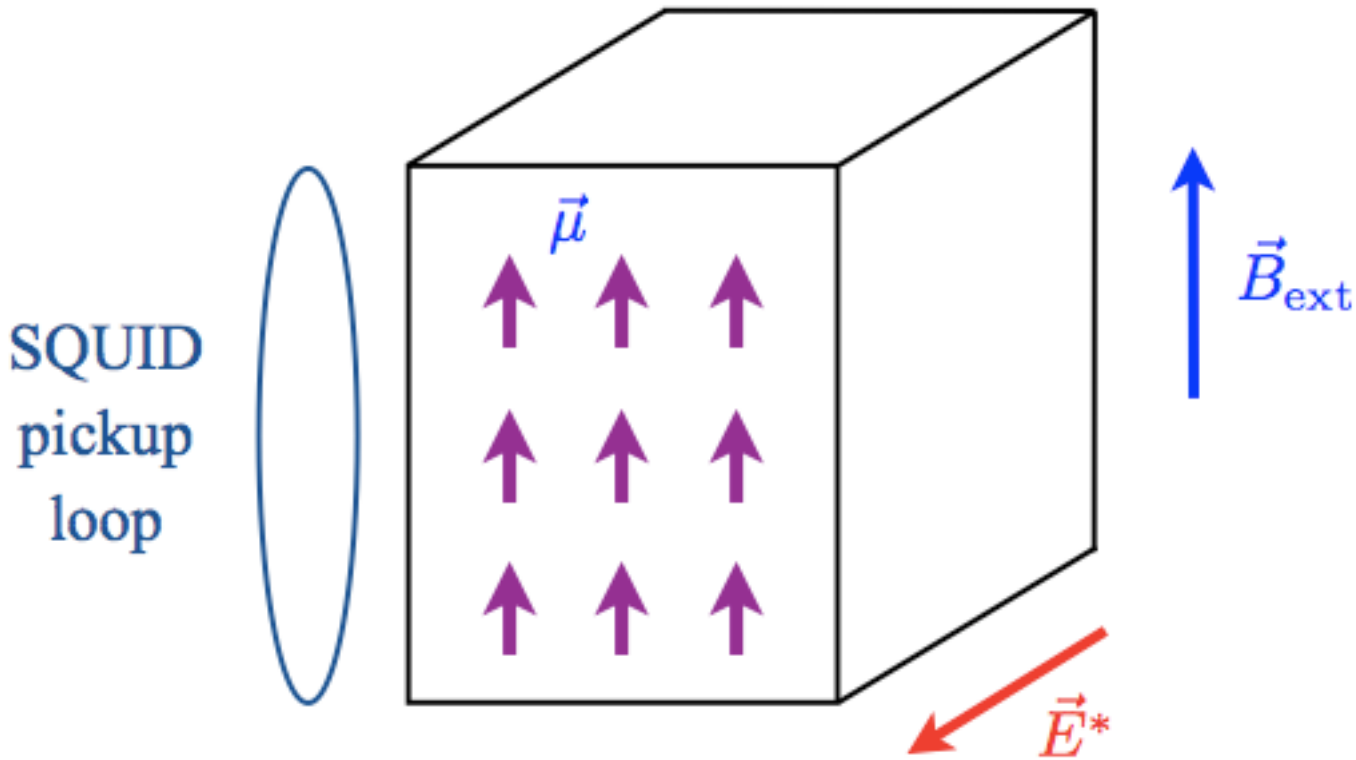

the axion field induces an oscillating nuclear electric di

$$d_e \sim 10^{-16}\ e\ \mathrm{cm}\ \frac{a(x)}{f_a}$$

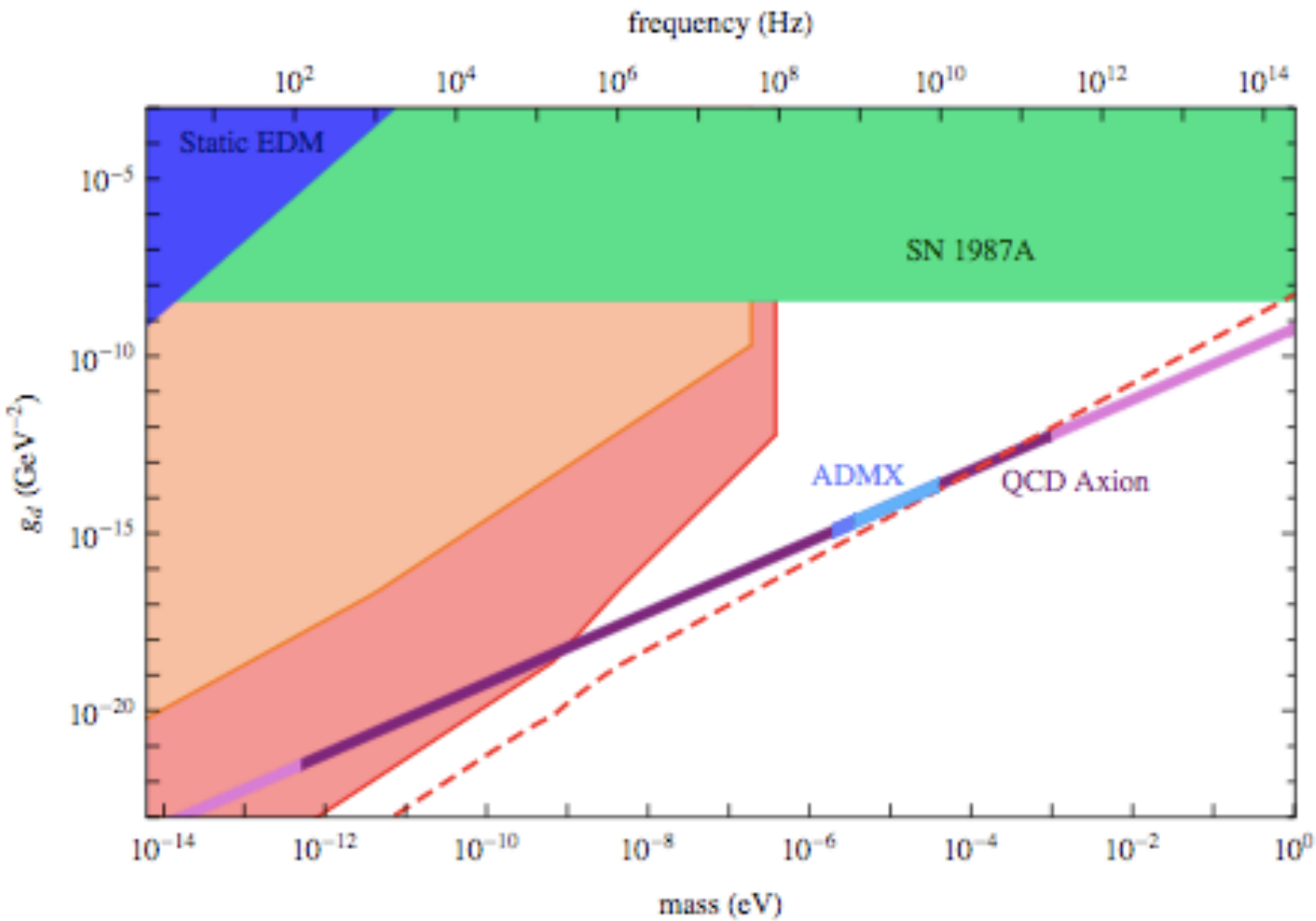

FIG. 2: Estimated constraints in the ALP parameter space in the EDM coupling g_d (where the nucleon EDM is $d_n = g_d a$ and a is the local value of the ALP field) vs. the ALP mass [17]. The green region is excluded by the constraints on excess cooling of supernova 1987A [17]. The blue region is excluded by existing, static nuclear EDM searches [17]. The QCD axion is in the purple region, whose width shows the theoretical uncertainty [17]. The solid red and orange regions show sensitivity estimates for our phase 1 and 2 proposals, set by magnetometer noise. The red dashed line shows the limit from magnetization noise of the sample for phase 2. The ADMX region shows what region of the QCD axion has been covered (darker blue) [34] or will be covered (lighter blue) [59, 60]. Phase 1 is a modification of current solid state static EDM techniques that is optimized to search for a time varying signal and can immediately begin probing the allowed region of ALP dark matter. To calculate limits from previous (static) EDM searches as well as our sensitivity curves, we assume the ALP is all of the dark matter.

Axion dark matter detection using an LC circuit

PS, D. Tanner and N. Sullivan, 2013

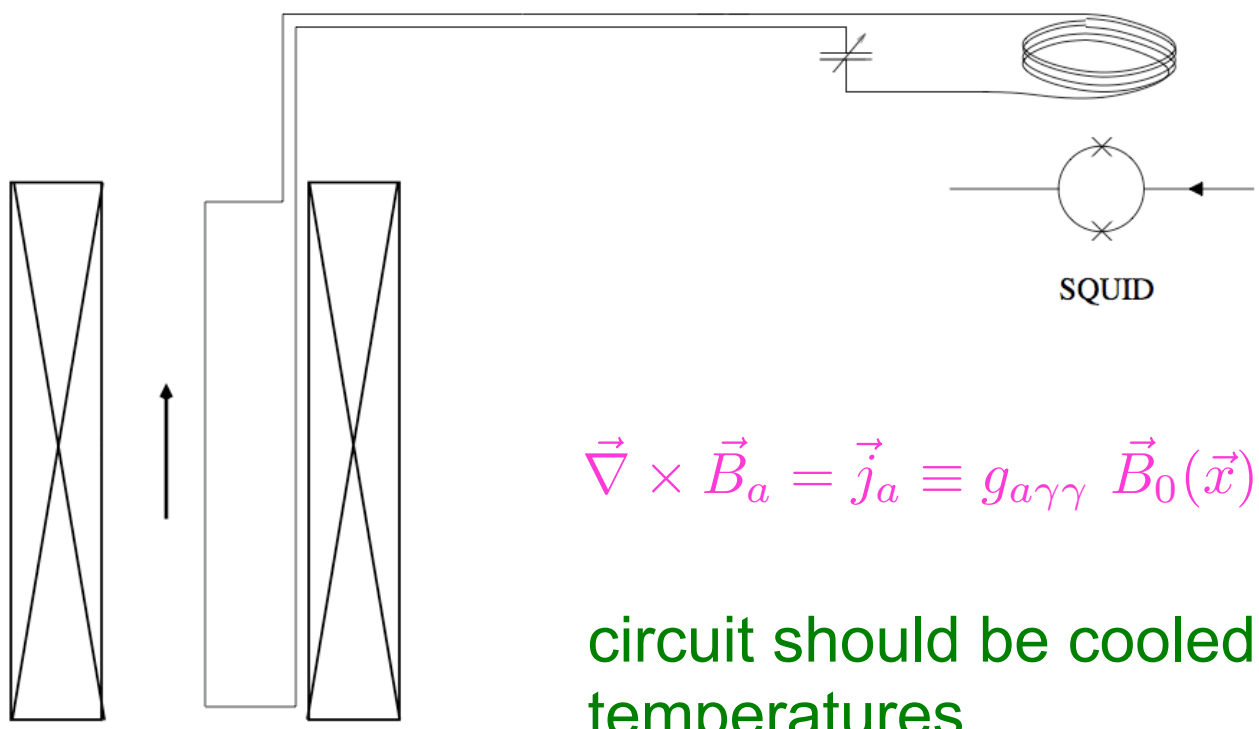

$$\vec{\nabla} \times \vec{B}_a = \vec{j}_a \equiv g_{a\gamma\gamma}\ \vec{B}_0(\vec{x})\ \partial_t a(\vec{x}, t)$$

circuit should be cooled to milli-Kelvin temperatures

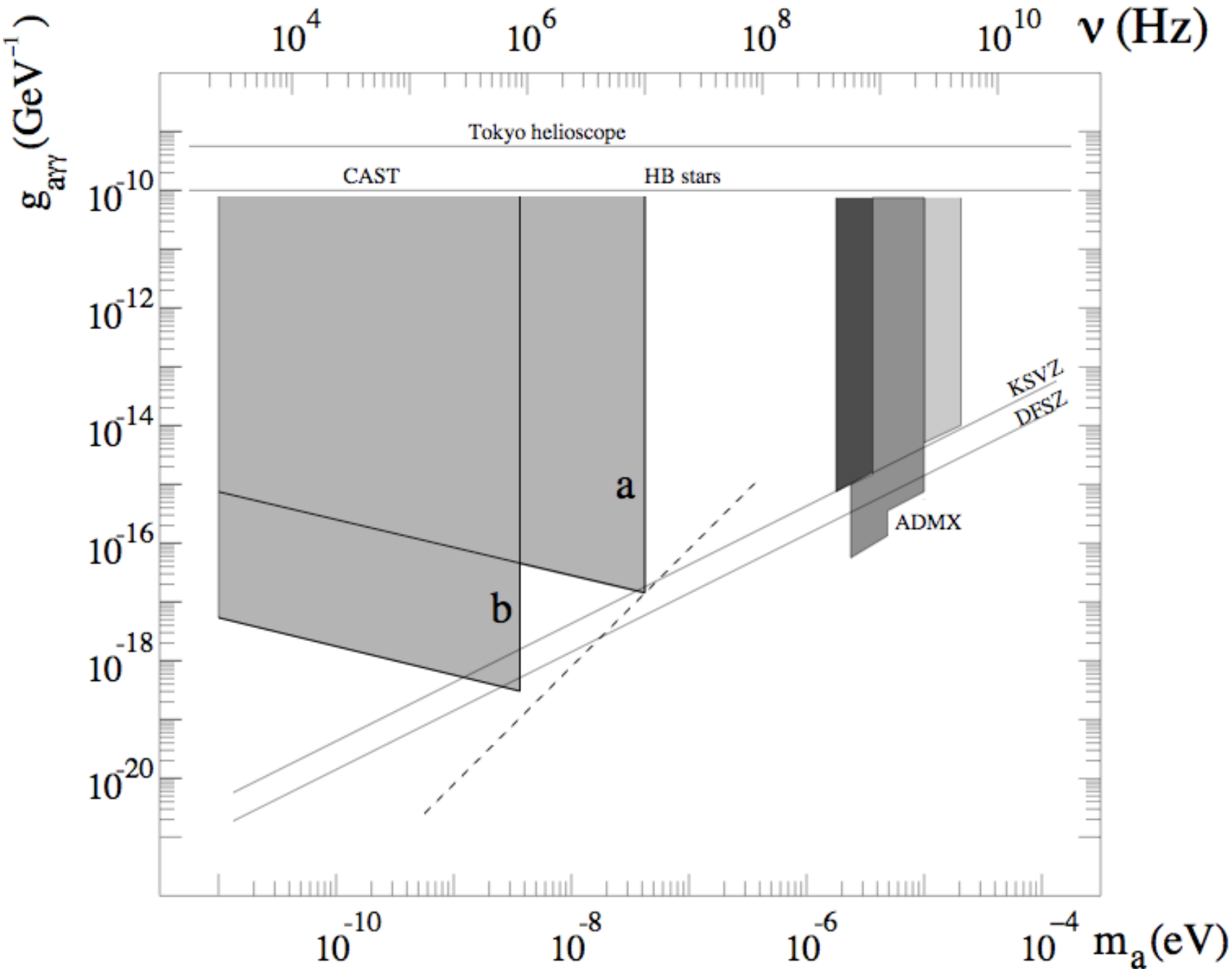
10^4
10^6
10^8
10^{10}
ν (Hz)
$g_{a\gamma\gamma}$ (GeV^{-1})
Tokyo helioscope
CAST
HB stars
10^{-10}
10^{-12}
10^{-14}
10^{-16}
10^{-18}
10^{-20}
a
b
KSVZ
DFSZ
ADMX
10^{-10}
10^{-8}
10^{-6}
10^{-4}
m_a(eV)

Axion dark matter detection using atomic transitions

PS 2014

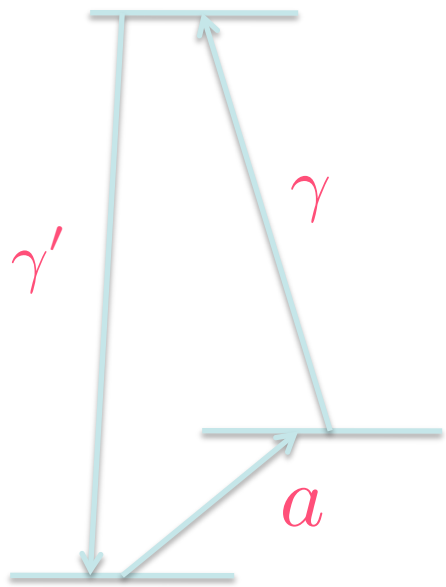

$$\mathcal{L}_{a\bar{f}f} = -\frac{g_f}{2f_a}\partial_\mu a(x)\bar{f}(x)\gamma^\mu\gamma_5 f(x)$$

$$f \text{ is electron, or nucleon}$$

$$H_{a\bar{f}f} = +\frac{g_f}{2f_a}\vec{\sigma}_f \cdot \vec{\nabla} a$$

- tune using the Zeeman effect
- use laser techniques to count axion induced transitions
- must cool to milli-Kelvin temperatures

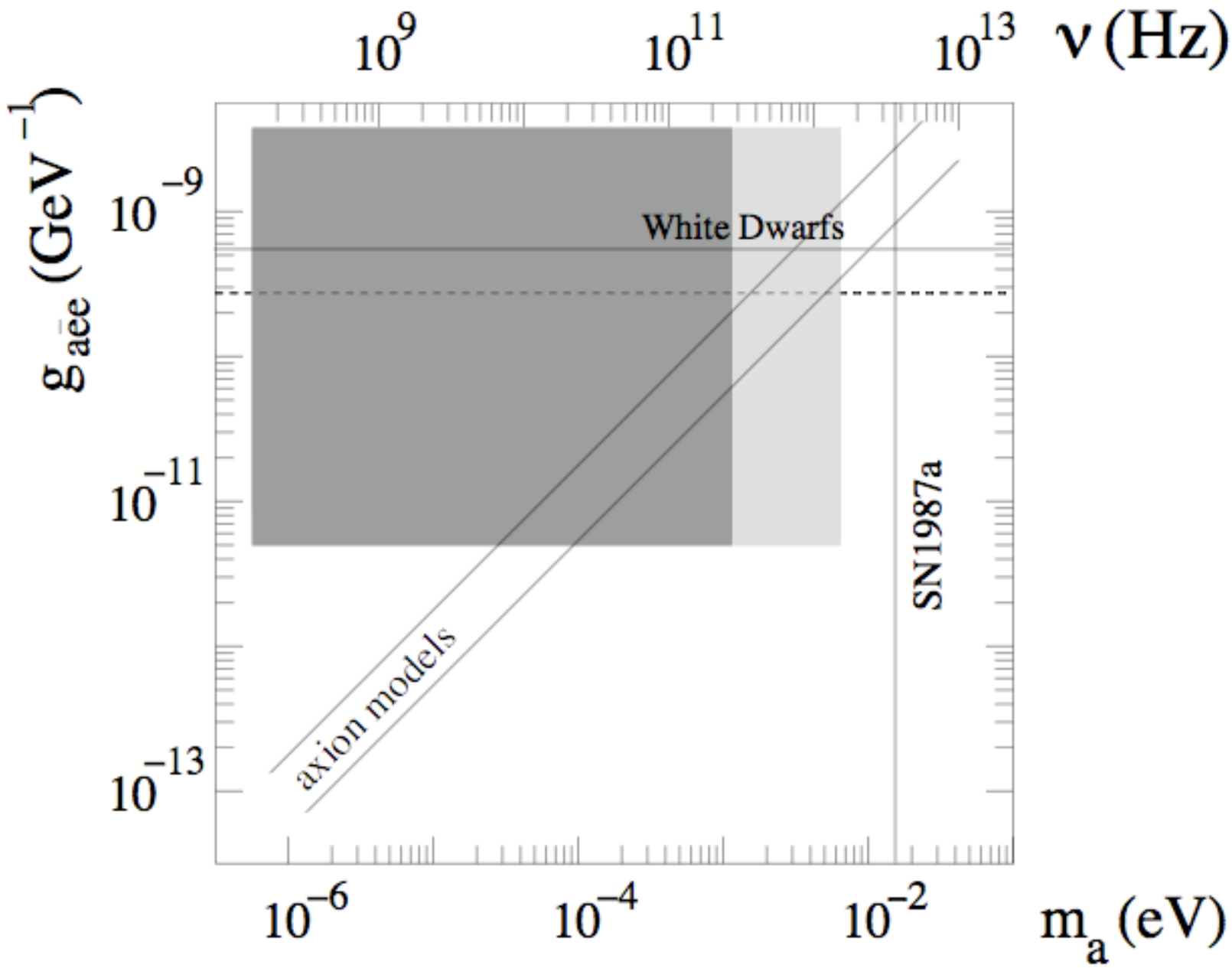
10^{9}
10^{11}
10^{13}
ν (Hz)
$g_{a\bar{e}e}$ (GeV^{-1})
10^{-9}
10^{-11}
10^{-13}
White Dwarfs
SN1987a
axion models
10^{-6}
10^{-4}
10^{-2}
m_a (eV)

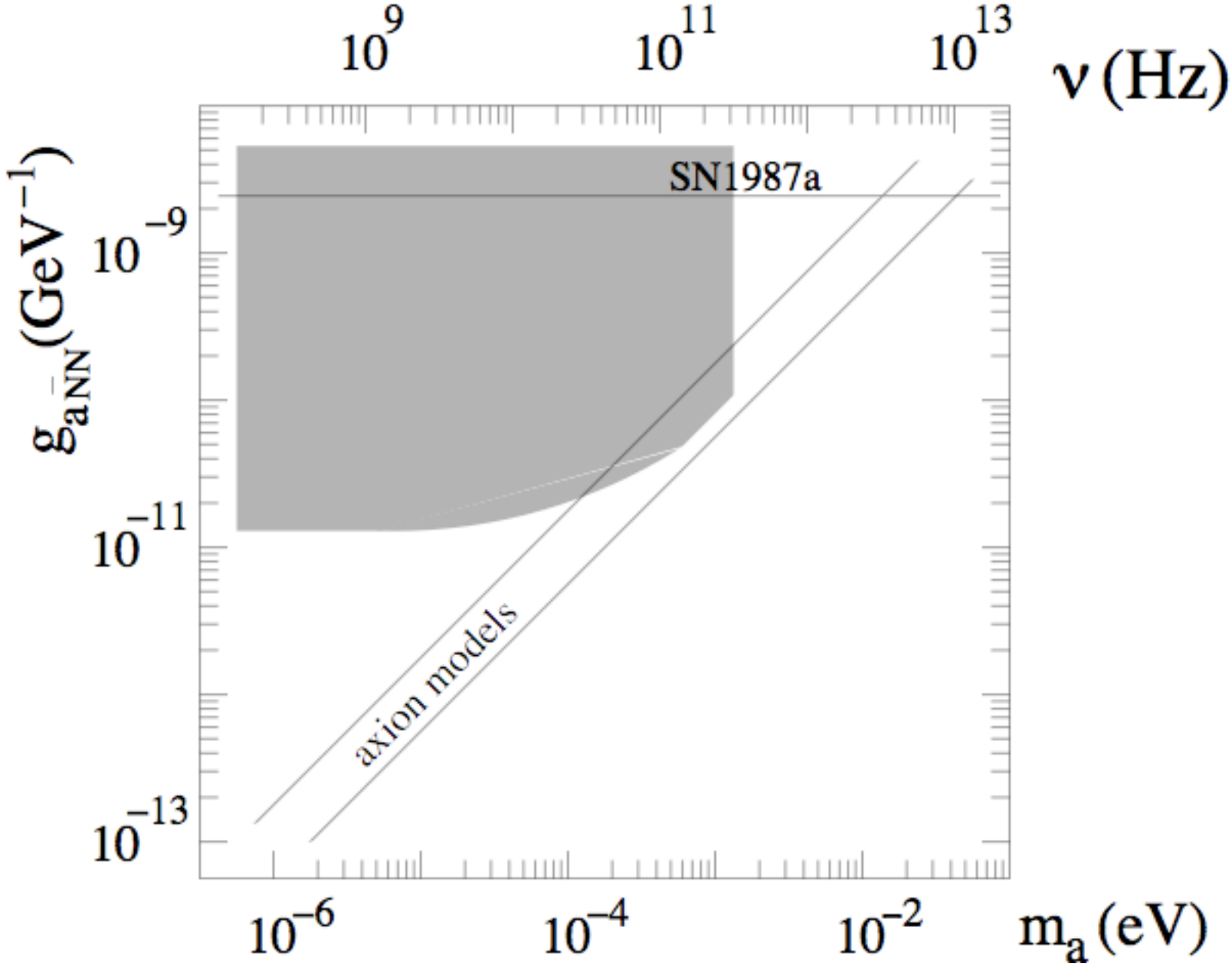
10^9
10^{11}
10^{13}
ν (Hz)
SN1987a
$g_{a\bar{N}N}$ (GeV^{-1})
10^{-9}
10^{-11}
10^{-13}
axion models
10^{-6}
10^{-4}
10^{-2}
m_a (eV)

Conclusions

- Axion dark matter is well motivated
- Axion dark matter can be detected over most of the plausible mass range